

REVIEW

An Invited Review for the Special 20th Anniversary Issue of MRMS

Advanced Diffusion MR Imaging for Multiple Sclerosis
in the Brain and Spinal Cord

Masaaki Hori^{1,2*}, Tomoko Maekawa², Kouhei Kamiya^{1,2}, Akifumi Hagiwara²,
Masami Goto³, Mariko Yoshida Takemura¹, Shohei Fujita², Christina Andica²,
Koji Kamagata², Julien Cohen-Adad⁴, and Shigeki Aoki²

Diffusion tensor imaging (DTI) has been established its usefulness in evaluating normal-appearing white matter (NAWM) and other lesions that are difficult to evaluate with routine clinical MRI in the evaluation of the brain and spinal cord lesions in multiple sclerosis (MS), a demyelinating disease. With the recent advances in the software and hardware of MRI systems, increasingly complex and sophisticated MRI and analysis methods, such as q-space imaging, diffusional kurtosis imaging, neurite orientation dispersion and density imaging, white matter tract integrity, and multiple diffusion encoding, referred to as advanced diffusion MRI, have been proposed. These are capable of capturing *in vivo* microstructural changes in the brain and spinal cord in normal and pathological states in greater detail than DTI.

This paper reviews the current status of recent advanced diffusion MRI for assessing MS *in vivo* as part of an issue celebrating two decades of magnetic resonance in medical sciences (MRMS), an official journal of the Japanese Society of Magnetic Resonance in Medicine.

Keywords: *diffusional kurtosis imaging, double diffusion encoding, multiple sclerosis, neurite orientation dispersion and density imaging, oscillating gradient spin-echo*

Introduction

Multiple sclerosis (MS) is a demyelinating disorder characterized by inflammatory demyelination accompanied by axonal degeneration that mainly affects young individuals. Some lesions undergo repair of injured myelin subsequently, while others may fail to repair and evolve into chronic plaques with variable degrees of chronic demyelination and axonal injury. Currently, there is no cure for MS, and the treatment focuses on hastening the recovery from the attacks, slowing the progression of the disease and managing the symptoms of MS. Corticosteroids, such as pulse steroid therapy and oral

prednisone, reduce nerve inflammation during MS attacks. Several disease-modifying therapies modify disease progression. Interferon β , fingolimod, natalizumab, glatiramer acetate, and dimethyl fumarate are disease-modifying drugs approved for use in Japan.¹

Conventional clinical MRI, including T1-, T2-, and fluid-attenuated inversion-recovery (FLAIR) imaging, has played an important role in the diagnosis and monitoring of the disease in clinical situations, as stated in the revised McDonald criteria.² However, the degree of disease progression in MS does not always coincide with the initial imaging findings.^{3,4} This has been explained by the normal-appearing white matter (NAWM), which has ongoing microstructural damage in neural tissues but does not show abnormal intensity on conventional MRI.

Diffusion tensor imaging (DTI) is a technique sensitive to the motion of water molecules *in vivo* and has been reported to be a useful tool in detecting abnormalities in the brain and spinal cord in patients with MS. Quantitative metrics of DTI, such as mean diffusivity (MD), which shows the rotationally invariant magnitude of the water molecule diffusivity within a voxel, and fractional anisotropy (FA), which shows the directionality of water molecule diffusion, have been widely used as a quantitative assessment index for NAWM and MS

¹Department of Radiology, Toho University Omori Medical Center, Tokyo, Japan

²Department of Radiology, Juntendo University School of Medicine, Tokyo, Japan

³Department of Radiological Technology, Faculty of Health Science, Juntendo University, Tokyo, Japan

⁴NeuroPoly Lab, Polytechnique Montreal, Montreal, Canada

*Corresponding author: Department of Radiology, Toho University Omori Medical Center, 6-11-1, Omorinishi, Ota-ku, Tokyo 143-8541, Japan. Phone: +81-3-3762-4151, Fax: +81-3-3768-5386, E-mail: masahori@med.toho-u.ac.jp



This work is licensed under a Creative Commons Attribution-NonCommercial-NoDerivatives International License.

plaques. Over 300 DTI papers have been published in the evaluation of MS to date.⁵ For instance, DTI parameters are abnormal within MS lesions showing increased diffusivity and reduced anisotropy on comparing with NAWM.^{6,7} These results are consistent with the increased water content, loss of myelin and axons, and the presence of gliosis. Moreover, abnormal DTI parameter values are frequently found in the NAWM of MS patients relative to age-matched controls, which contribute to the establishment of widespread white matter damage, even in the early phases. However, DTI metrics lack specificity as indicators of pathological changes. For instance, decreased FA is a common finding in the white matter of MS patients, but it is not specific, as it can be caused by a variety of factors, including the decreased density of neurites and decreased myelin. There are limitations in evaluating FA alone, and FA cannot distinguish between diseases characterized by pathological processes, such as edema, inflammation, demyelination, and leukoaraiosis.⁸ Therefore, several advanced and complex diffusion MR imaging (dMRI) and analyses have been introduced in the last two decades to capture more specific pathological changes. There is a review that suggests that multiple advanced dMRI is a quantitative MRI method with high sensitivity and specificity for the evaluation of MS lesions and NAWM.⁹

In this review, we describe the recent advances in dMRI in assessing MS *in vivo*.

Q-Space Imaging

Q-space imaging (QSI) is an analytical method for diffusion MRI using high b-values. It can calculate the average distance traveled and the probability density map of water molecules in one voxel during a given diffusion time from the MRI data with multiple and high b-values (Fig. 1). QSI does not introduce the assumption of Gaussian diffusion in the calculation of quantitative values, which acts as an advantage, while DTI assumes Gaussian diffusion of water molecules. In DTI, the Einstein–Smoluchowski equation,

$$\langle x^2 \rangle = 2Dt$$

where $\langle x^2 \rangle$ = mean square displacement, D = the diffusion coefficient, t = the diffusion time, acts as the basis for the diffusion tensor image, and it is assumed that water molecules exhibit Gaussian diffusion. However, there is a discrepancy in the actual water movement in neuronal tissues *in vivo*. In a living organ, there is a 3D partition or compartmental structure composed mainly of cells and other structures, and water molecules collide with obstacles immediately after initial movement. Therefore, the assumption that diffusion is normally distributed is not true in most cases *in vivo*. However, compared to conventional DTI, QSI is not as widely used in clinical practice since it requires a large number of high b-values established by limited high-performance MRI systems. Moreover, it requires a long

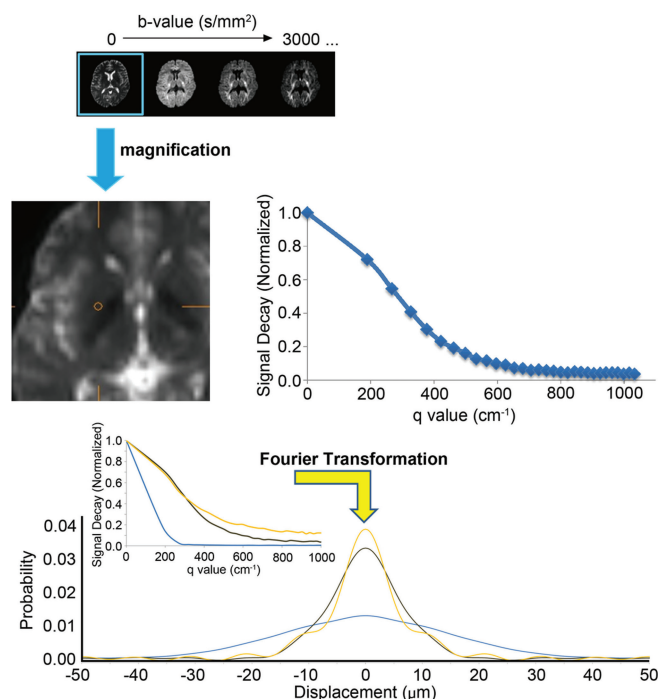


Fig. 1 The process of QSI metrics from DWI data set. First, a DWI dataset with multiple b- (q-) values of up to approximately 10000 s/mm² is acquired. A q-value signal intensity curve is obtained for each pixel. After the Fourier transformation of the signal decay with respect to q producing a non-Gaussian displacement distribution profile for each pixel, probability density function curves are calculated. The mean displacement (calculated from the full width at half height) and the probability for zero displacement (given by the height of the profile at zero displacement) are important indices. The yellow line indicates white matter, the gray line indicates gray matter, and the blue line indicates cerebrospinal fluid (adapted from Fig. 1 of reference #17). DWI, diffusion-weighted imaging; QSI, q-space imaging.

imaging time. In addition, its application in humans is relatively older than that of DKI, which was introduced later and reported on by Assaf et al.¹⁰ and Cohen et al.¹¹ in 2002. The maximum b-value in these studies was 14000 s/mm². In these early reports, QSI was found to be very sensitive to MS lesions compared with conventional MRI, especially in the NAWM of the brains with MS. A more detailed study showed that QSI correlated with N-acetylaspartate levels measured by MRS and was useful in detecting abnormalities in NAWM in MS.¹² One QSI study using a maximum b-value of 6400 s/mm² showed the potential to assess different cerebral water components and plaques of different degrees of demyelination showed different features in MS patients.¹³ In spinal cord MS lesions, Farrell et al.¹⁴ showed the usefulness of QSI analysis as a feasibility study. The mean displacement of water molecules, one of the metrics of QSI analysis, similar to the apparent diffusion coefficient (ADC) of the diffusion tensor analysis, showed higher values in NAWM and MS plaques (Fig. 2).^{15,16} In general, the

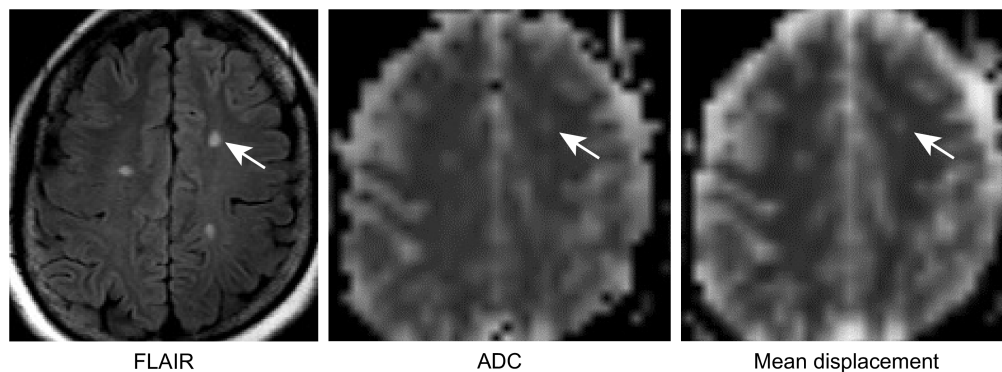


Fig. 2 Images from a patient with MS. FLAIR image shows the demyelinated lesions as abnormal hyperintensity spots. The corresponding map of ADC from a DTI analysis and a mean displacement map from a QSI analysis show the lesions as abnormally high values compared with surrounding white matter. ADC, apparent diffusion coefficient; DTI, diffusion tensor imaging; FLAIR, fluid-attenuated inversion recovery; QSI, q-space imaging.

advantage of QSI compared to DTI is its ability to detect pathologic conditions with higher sensitivity.^{17,18} Moreover, QSI-based myelin imaging was introduced to monitor demyelination and remyelination in MS patients.^{19–22} It is important to note that advanced diffusion analysis in the spinal cord and brain has been performed *in vivo*,^{23–25} demonstrating that it is possible to observe microstructural changes in the spinal cord in patients with MS.

Diffusional Kurtosis Imaging

Diffusional kurtosis imaging (DKI) is closely related to QSI. QSI methods have been employed to estimate diffusional kurtosis as a metric derived from QSI analyses.¹³ DKI was established by Jensen et al.²⁶ as a method to quantify the deviation from a Gaussian distribution. According to this report, the relationship between diffusivity (D), diffusional kurtosis (K), and the signal in the diffusion-weighted image is expressed using the following equation:

$$\ln[S(b)/S_0] = -bD + \frac{1}{6}b^2D^2K$$

where b = b value (s/mm^2), $S(b)$ is the signal intensity at b , and S_0 is the signal intensity at b value of 0. This formula is an expansion of the DTI (Fig. 3).

The merit of DKI compared to QSI is that it can be calculated with lesser MRI data than QSI and is easier to apply in clinical situations. In a minimal DKI protocol, an image dataset consisting of two b -values (such as $b = 1000$ and $2000 s/mm^2$) is often used in addition to the $b = 0$ image. Numerous motion probing gradient axes (usually 15 or more axes) are required for DKI than for DTI, but a realistic imaging time is possible for clinical application. However, in early reports of DKI, some studies did not cover the whole brain as the imaging range,²⁷ and a reasonable imaging time

could be achieved by methods such as the simultaneous multi-slice technique that shortens the imaging time.^{28–30} The advantage of DKI compared to DTI is that white matter damage in MS patients, especially hidden microstructural abnormalities in NAWM, can be detected with greater sensitivity by quantitative values obtained from DKI, such as the mean kurtosis.^{31,32} Moreover, the mean kurtosis obtained from DKI has the advantage of being less susceptible to crossing fibers, unlike FA (Fig. 4). Therefore, an accurate evaluation of NAWM in the whole brain can be expected using DKI. In addition to the brain, the usefulness of DKI has also been shown in the spinal cord in patients with MS.^{17,33} However, Martin et al.³⁴ described some skepticism regarding the usefulness of DKI in the spinal cord. It is difficult to argue that the most robust diffusion MRI technique for assessing past spinal abnormalities is the FA calculated from DTI. The number of studies evaluating the spinal cord using DKI at this stage is small, and more studies with a larger number of patients are needed to establish a base of evidence. Furthermore, studies on the brain have reported abnormalities in MS patients, such as microstructural changes in images, and correlated various clinical indices with metrics calculated from DKI. Bester et al.³⁵ showed that decreased cortical mean kurtosis was correlated with poor performance on cognitive tasks. A notable aspect of this study is that DKI was used to assess gray matter rather than white matter. Takemura et al.³⁶ found that the lateral geniculate nucleus may compensate for unilateral damage in the pregeniculate optic pathway via neural plasticity by using DKI and visual-evoked potentials. Spampinato et al.³⁷ showed that radial kurtosis of the corticospinal tract, which is kurtosis perpendicular to the main nerve fiber direction in the voxel, may be associated with neurological disability in MS patients.

DKI is also being applied in neuromyelitis optica (NMO), a clinically similar disease often misdiagnosed as MS on conventional MRI.^{38,39} Technically, the study of MS patients

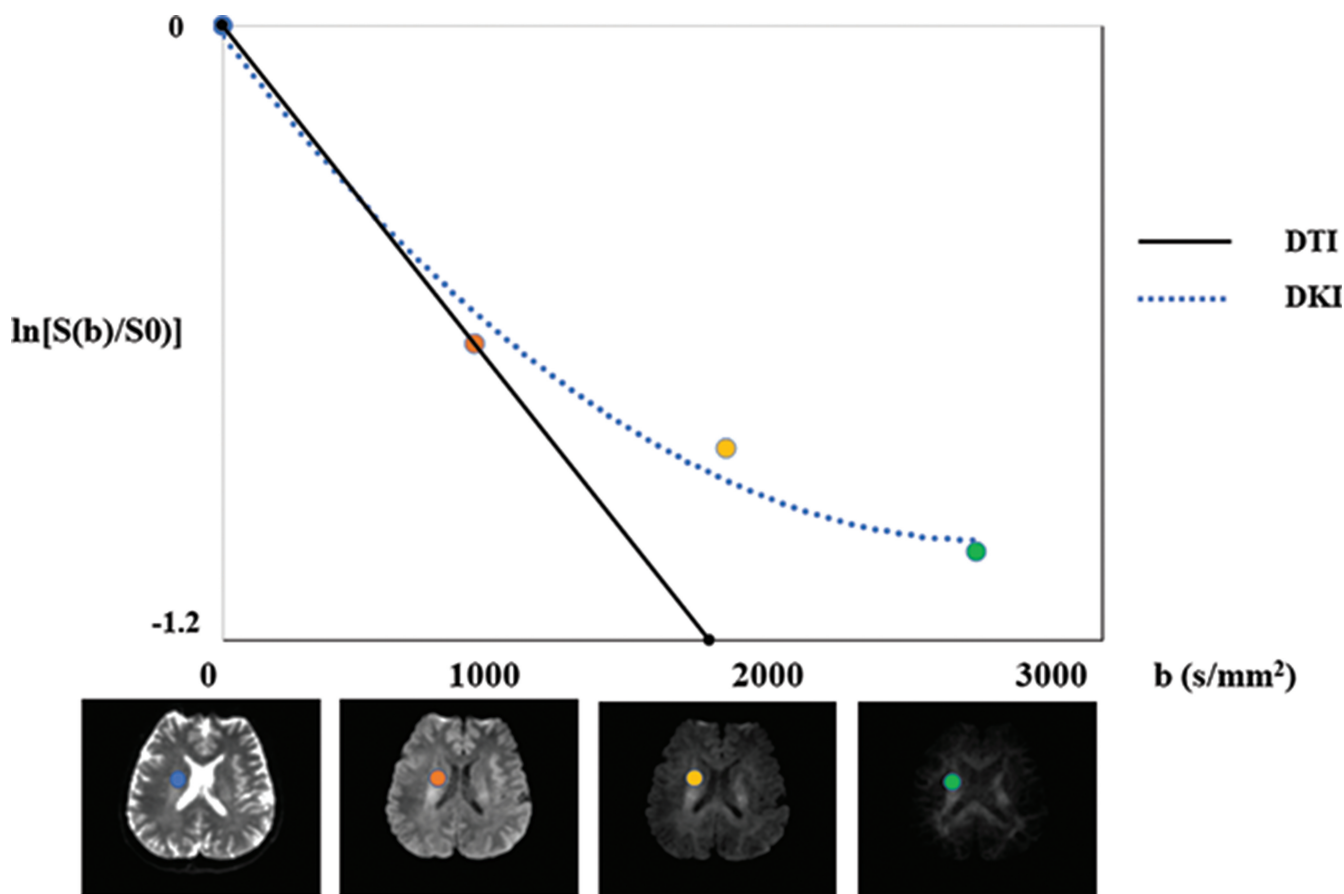


Fig. 3 Brief description of DKI and DTI signal fitting. The logarithm of normalized signal intensity of DWI (color dots) at b values of 0 and 1000 s/mm^2 is fitted to a black line for DTI. The logarithm of normalized signal intensity of DWI at multiple b-values is fitted to parabola for DKI. DKI, diffusional kurtosis imaging; DTI, diffusion tensor imaging; DWI, diffusion-weighted imaging.

in 7T MRI systems, which are expected to be widely used in the future, has already begun.⁴⁰ In addition, the usefulness of DKI with an imaging time of less than 3 minutes that utilizes a particular data collection method has been reported, although further reductions in the imaging time of DKI may be necessary for widespread use in clinical practice.⁴¹ One caveat regarding DKI is that kurtosis indicates the degree of deviation from the Gaussian distribution, and the value of kurtosis in diffusion MRI is thought to reflect the complexity of biological tissues to some extent; however, the interpretation of the value itself should be done carefully, and data from a large number of cases should be studied to establish its clinical usefulness. In addition, values such as mean kurtosis are not specific.

Neurite Orientation Dispersion and Density Imaging

From the viewpoint of modeling,⁴² DTI and DKI can be considered as numerical representations that aim to summarize or compress the information contained in the data without

detailed knowledge regarding the substrate itself. In contrast, NODDI⁴² belongs to the category of biophysical models⁴³ that aim to infer specific microstructural properties of biological tissue (e.g., neurite density).⁴⁴ Among several models proposed thus far, neurite orientation dispersion and density imaging (NODDI) is arguably the most popular model in clinical research at present.⁴⁵ NODDI assumes three compartments: intraneurite, extraneurite, and cerebrospinal fluid (CSF) (free water). The respective fractions for each of these were calculated as quantitative values. In addition, orientation dispersion, a measure that indicates the orientation of structures (such as axons and dendritic spines) in a voxel, was also calculated. The dMRI data required for the analysis of NODDI are approximately the same as those of DKI and less than those of QSI. In addition, it is possible to analyze both DKI and NODDI from the same data. Several studies on patients with MS have evaluated MS lesions and NAWM using NODDI.^{46–56} Moreover, NODDI has also been applied to spinal cord evaluation.^{57,58} A common finding in these studies is the reduction in intraneurite volume fraction (INVF) in the plaques of MS patients. In addition, there

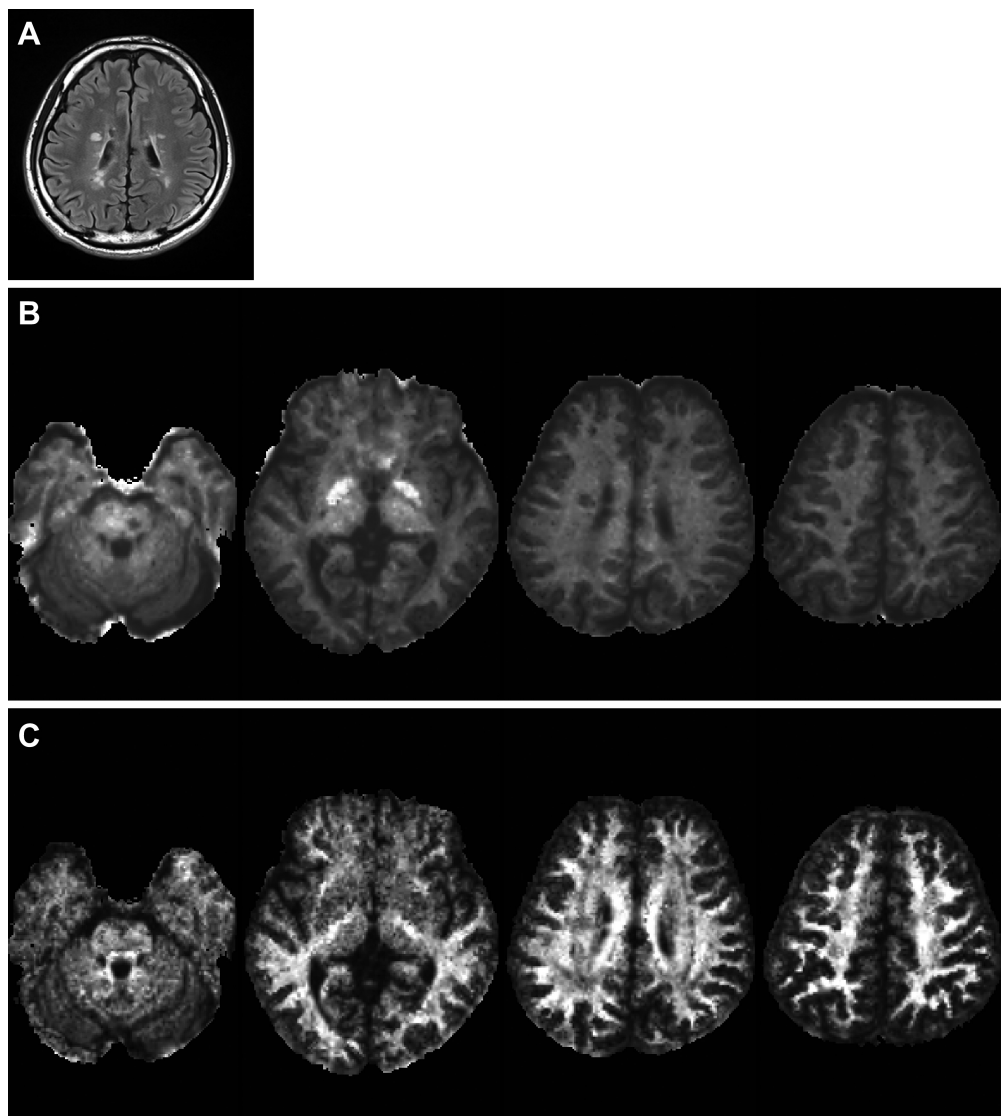


Fig. 4 FLAIR image (a) shows hyperintense lesions in deep white matter, indicating MS plaques. Mean kurtosis maps (b) and FA maps (c) show the plaques as hypointense lesions. Note that, in the mean kurtosis map, white matter can be assessed without the influence of crossing fibers. FA, fractional anisotropy; FLAIR, fluid-attenuated inversion recovery.

was a decrease in INVF in the NAWM, though not as much as in the above demyelinated foci. These changes captured by NODDI are more widespread than those observed by DTI and conventional MRI techniques, suggesting that NODDI is an excellent method for evaluating microstructural changes. Pathologically, a decrease in INVF in NODDI suggests neurite degeneration and decreased density associated with chronic or progressive nerve demyelination in MS. However, it should be noted that the results with orientation dispersion (OD), one of the indices calculated from NODDI, have not been consistent in MS patients. Grussu et al.⁵⁹ showed decreased OD in MS lesions and excellent agreement between the orientation dispersion index and its histological counterpart in a postmortem spinal cord study.

However, there are some caveats regarding the use of NODDI in clinical research. The analysis of diffusion MRI using a model such as NODDI may not always fit correctly in tissues under pathological conditions.⁴⁵ Further studies with more clinical cases and comparisons with histopathology, clinical symptoms, and prognosis are needed to confirm this. In addition, the quantitative metrics calculated by NODDI vary depending on the imaging conditions, although clinicians are not particularly aware of it.⁶⁰ Diffusion time dependence and TE dependence on diffusion MRI exist and affect the quantitative values, which is not limited to NODDI.^{61–65} Therefore, the above validity should be confirmed when the parameters calculated using NODDI are used as biomarkers in actual clinical cases.

White Matter Tract Integrity

White matter tract integrity (WMTI)⁶⁴ is another popular biophysical model that can be applied to the same data acquired for DKI and NODDI. WMTI is a two-compartment model (intra- and extra-axonal compartments) and is based on an analytical solution that directly links the kurtosis tensor to the model parameters (intra- and extra-axonal compartmental diffusion tensors and the axonal water fraction [AWF]). Subsequently, this analytical solution was extended to general situations (arbitrary fiber orientation distribution and the existence of a free water compartment) to elucidate the acquisition requirements for solving the general model. Enthusiastic readers are referred to previous publications on this topic.^{66,67} WMTI has been applied in clinical studies of MS,^{68–71} and these studies suggested that a decrease in AWF in the white matter correlates with clinical disability, presumably reflecting chronic axonal loss. In animal models, WMTI has been shown to be capable of distinguishing different tissue pathologies in demyelinating lesions and tracking their longitudinal courses. Specifically, extra-axonal radial diffusivity is related to the g-ratio,⁷² while AWF is linked to the axonal fraction derived from electron microscopy, which is in agreement with computer simulations of diffusing molecules.⁷³ In a cuprizone mouse model, intra-axonal axial diffusivity was observed in the acute phase, presumably reflecting axonal swelling or beading.⁷⁴ While NODDI and WMTI have their pros and cons, a distinguishing feature between the two is the estimation of compartmental diffusivities. Robust estimation of compartmental diffusivities has been a long-desired goal^{66,75} and is not yet possible in clinical situations, which is partly because the compartmental diffusivities affect the dMRI signal only marginally under the condition that SNR values and b-values are within the clinically available range. A common approach is to fix such parameters to reasonable values for the stable estimation of the others. Nonetheless, the compartmental diffusivities and their dependence on diffusion time would yield indispensable information regarding axon morphologies and demyelination,^{76–78} and extend the parameter space of dMRI biophysical models (multiple diffusion encoding, diffusion relaxation, and diffusion time), as discussed in the following paragraphs, which are promising avenues for future research.

Double Diffusion Encoding

The dMRI methods described above are all single diffusion encoding methods, despite the differences in b-values and the number of motion probing gradient (MPG) axes,^{79,80} which apply only one MPG in one direction and one size per encoding. The double diffusion encoding (DDE) pulse sequence,^{81,82} a method that applies two MPGs per encoding, has recently become available as a part of multiple

encoding technique. DDE allows the anisotropy to be measured in a single voxel and the microstructure of the individual elements comprising the voxel, which is quantified by the microscopic fractional anisotropy (μ FA) metric. DDE makes it possible to observe tissue microstructure *in vivo*, which differs from FA obtained by conventional DTI analysis and is expected to be clinically useful in the future. The first method proposed for the application of DDE in humans was quite long.⁸³ Subsequently, Yang et al.⁸⁴ proposed an imaging protocol for DDE that can be performed in 5 minutes in a clinical setting using data thinning during imaging. They showed that the μ FA maps showed improved delineation of MS lesions in the brain compared with conventional fractional anisotropy derived from DTI. Notably, the lesions displayed focal hypointensities on the μ FA map but not on the T2-FLAIR images in one patient. This was a feasibility study with a small patient number; however, the μ FA derived from DDE showed the potential to be a promising tool in the evaluation of MS *in vivo*. Further extension of diffusion encoding methods includes triple diffusion encoding⁸⁵ and more flexible arbitrary gradient waveforms.⁸⁶ Such arbitrary waveforms enable a more time-efficient protocol than DDE (under the assumption of multiple Gaussian compartments), and promising results have been reported in a recent clinical study of MS.⁸⁷

Combination of MR Myelin Imaging and Advanced dMRI

Various methods of myelin imaging using MRI have been proposed^{88–90} and are expected to be clinically useful in MS, a demyelinating disease, and correlate with a variety of clinical indices. However, the details of myelin imaging are beyond the scope of this study.

Recently, MR fiber g-ratio (the ratio of the diameter of the axon to the diameter of the neuronal fiber) mapping was introduced for the brain^{91–93} and spinal cord.^{94,95} For MR fiber g-ratio mapping, two quantitative MR measurements, quantitative myelin mapping for the myelin volume fraction (MVF) and quantitative axon mapping, which are usually metrics derived from dMRI for the axon volume fraction (AVF), were used to calculate the aggregate g-ratio in a voxel. The MR g-ratio is expected to be a promising method for the quantitative evaluation of the degree of myelination or axonal damage *in vivo*, which is difficult to evaluate with conventional MRI. The g-ratio was directly visualized and measured using electron microscopy.⁹⁶ A previous autopsy study of brains reported dynamic g-ratio changes in demyelinating diseases, such as MS.⁹⁷ The g-ratio is related to the neuron conduction velocity.⁹⁸ Lesions with pure demyelination have an increased g-ratio. In contrast, lesions with concomitant myelin and axonal loss demonstrate an unchanged or increased g-ratio. We analyzed MVF, AVF, and MR g-ratio values in MS patients and showed that myelin is more damaged than axons in plaques and periplaque white matter

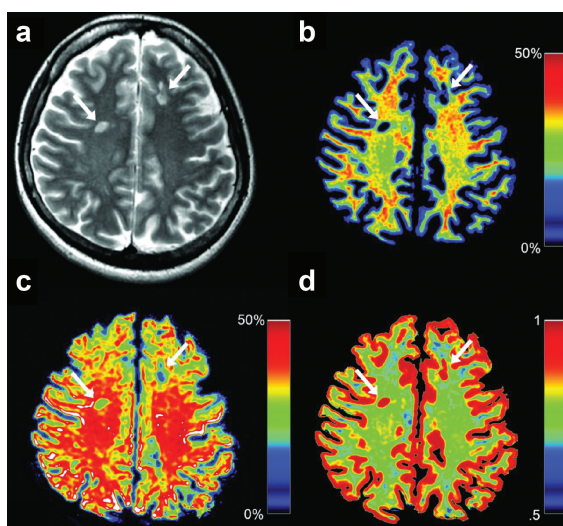


Fig. 5 Representative images from a patient with MS. Synthetic T2WI (a) and maps of myelin volume fraction (b), axon volume fraction (c), and g-ratio (d) are shown. Two plaques are designated by arrows in these images. The myelin is severely damaged in these plaques (b, 5.53% and 7.23%); however, the degrees of axon damage are milder (c, 31.30% and 22.95%). Since the myelin is severely damaged in these plaques, the corresponding g-ratios are close to 1.00 (d, 0.94 and 0.91) (adapted from Fig. 1 of reference #48). T2WI, T2-weighted imaging.

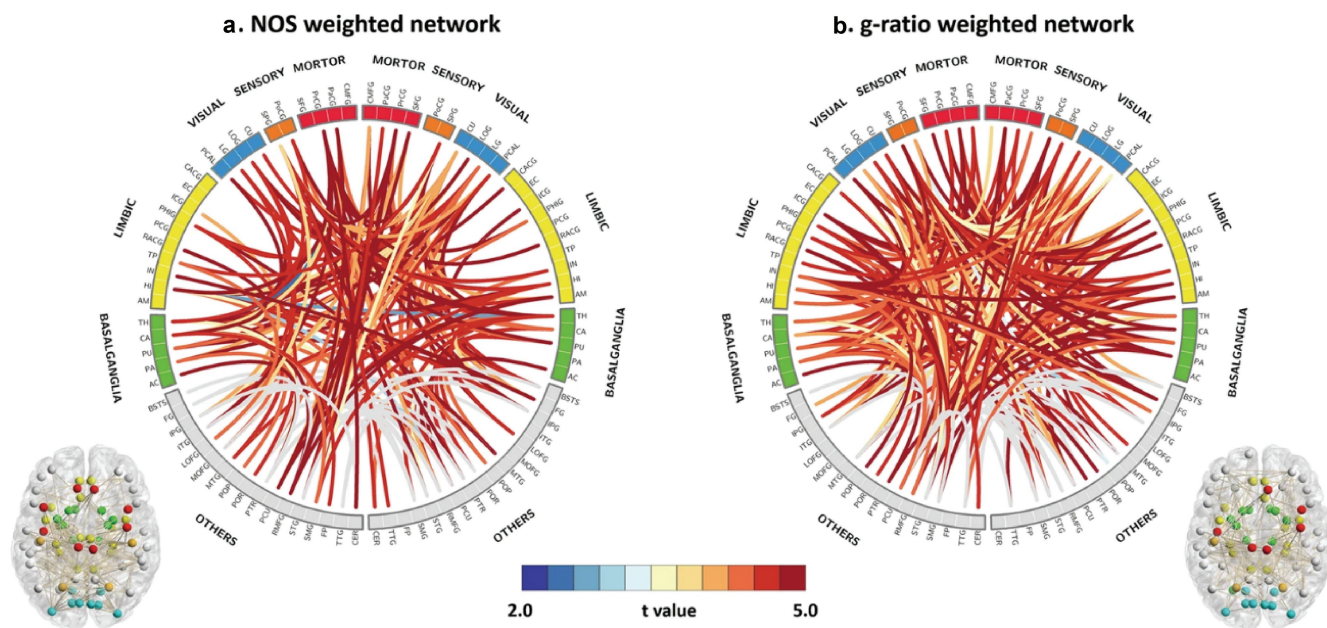


Fig. 6 Comparison of subnetworks with significantly altered connectivity in each network. (a) Subnetworks with significantly decreased NOS-weighted connectivity in patients with MS versus controls. (b) Subnetworks with significantly increased g-ratio-weighted connectivity in patients with MS versus controls (see correspondence of abbreviations with anatomical regions in Supplementary Table S5 of reference #99) (adapted from Fig. 2 of reference #99). MS, multiple sclerosis; NOS, number of streamlines.

of patients with MS.⁴⁸ Thus, these imaging methods could be used as a measure of myelination, demyelination, and remyelination, which cannot be discriminated using conventional MRI in demyelinating diseases, such as MS (Fig. 5). An advanced study involved the application of the MR g-ratio to structural connectome analysis.⁹⁹ In this study, Kamagata et al.⁹⁹ compared the network topology of the brain in MS patients using MR g-ratio-weighted analyses and normal

network analyses. The authors found that the g-ratio-weighted nodal strength in the motor, visual, and limbic regions significantly correlated with interindividual variation in measures of disease severity (Fig. 6). The g-ratio determines the neuron conduction velocity^{98,100} and influences normal brain functions;¹⁰¹ therefore, network analysis using the MR g-ratio could be a potential biomarker that more accurately reflects the state of the brain network.

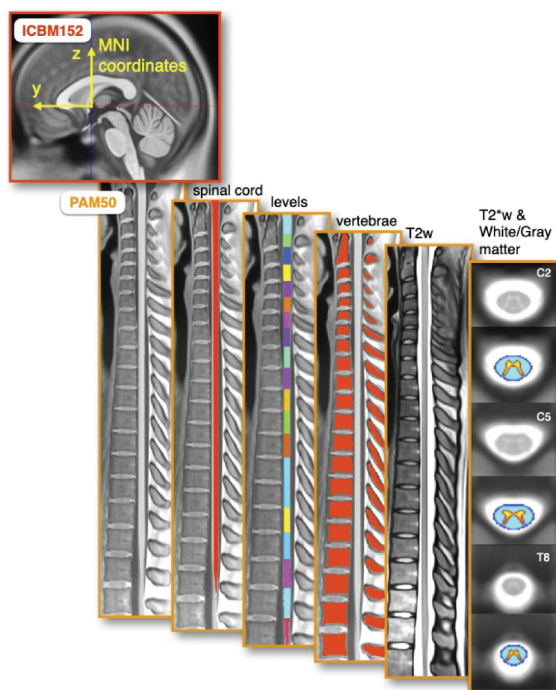


Fig. 7 PAM50 MRI template of the full spinal cord and brainstem. The PAM50 template is compatible with the ICBM152 brain template (the MNI template), allowing researchers to conduct simultaneous brain/spine studies within the same coordinate system. The PAM50 template includes atlases of white matter pathways, gray matter subregions, and probabilistic spinal levels (adapted from <https://spinalcordtoolbox.com>, with permission).

Notes for Spinal Cord Imaging Analysis

Advanced dMRI has recently been applied and studied *in vivo* in the brain and spinal cord. However, a problem with MRI studies of the spinal cord in the past was that, unlike the brain, there was no standardized method or software for analyzing any quantitative maps. As a result, quantitative values in past MRI studies of the spinal cord were often created by ROIs, and arbitrariness could not be completely eliminated. Currently, well-known and objective tools for quantitative evaluation, such as statistical parametric mapping software (SPM, www.fil.ion.ucl.ac.uk/spm/software/) and the FMRIB software library (FSL, www.fmrib.ox.ac.uk/fsl/index.html), are widely used for advanced dMRI of the brain, and many templates can automatically set up anatomical ROIs in standard space.^{102,103} Thus, the recent release of the Spinal Cord Toolbox (SCT)¹⁰⁴ (this software can be downloaded and installed free of charge from the following link: <https://spinalcordtoolbox.com>), for objective measurement and evaluation in the spinal cord, is considered to be of great significance. The functions of SCT include spinal cord segmentation in the image, motion correction of diffusion MRI of the spinal cord, and registration to the template¹⁰⁵ (Fig. 7). This template of normal white matter and gray matter enables objective analyses. For instance, if the study investigated the spatial distribution of MS lesions in MRI images of the spinal cord from multiple centers with different imaging protocols, the problem of differences in protocols between centers (i.e., differences in spatial

resolution and slice thickness) can be resolved by aligning the MRI images on this template.

The spinal cord has the same white matter and gray matter structures as the brain, but there is some debate as to whether it is appropriate to apply the same dMRI analysis methods used in the brain to the spinal cord. In humans imaged using current MRI systems, only the cranio-caudal direction nerve fibers can be depicted, taking into account the spatial resolution and other various conditions. In addition, it is difficult to obtain good image quality since spinal cord imaging is more easily affected by surrounding structures, such as bone and air, and physiological movements (breathing, etc.). Therefore, taking these factors into consideration, a dMRI imaging and analysis method that is more suitable and specific to the spinal cord is desired in the future.

Future Perspective for Advanced dMRI

Recently, an oscillating gradient spin-echo (OGSE) sequence has become available in clinical MRI scanners.^{106–109} OGSE can shorten the diffusion time by replacing the long diffusion-sensitizing gradients used in pulsed gradient spin-echo (PGSE) sequences with rapidly oscillating gradients. DWI with OGSE sequence enables short diffusion times and allows us to explore time dependencies that are not accessible to the PGSE sequence. OGSE sequences are expected to provide insight into the internal structures of pathologic lesions based on the analysis of changes in ADC values with different diffusion times. Clinically, acute ischemic stroke,¹¹⁰

intracranial epidermoid cysts,¹¹¹ transient splenial lesions,¹¹² head and neck tumors,¹¹³ breast tumors,¹¹⁴ and prostate cancer¹¹⁵ have been analyzed using DWI with OGSE sequence. OGSE sequences may be useful in evaluating the internal structure of lesions and differentiating between benign and malignant tumors. No studies have evaluated the brain and spinal cord of MS patients using OGSE sequences, but there is a preliminary study that evaluated the spinal cord of two MS patients using an OGSE sequence.¹¹⁶ OGSE sequences may be used to evaluate the microstructure of the brain and spinal cord of MS patients and may provide us with new insights. In addition, an important key concept with OGSE is the diffusion time dependence. In dMRI using SDE in conventional MRI systems, TE and diffusion time are almost automatically set once the b-value is determined. Preclinical studies have reported that the differences in the diffusion-weighted images and the quantitative values obtained from the dMRI data due to the diffusion time provide various types of new information on the microstructure of the body. For instance, a correlation with abnormal mitochondria in MS has been reported in human studies.

Other future advances in diffusion MRI include the development of more complex models and analysis methods. For instance, a compartment-based model for noninvasive apparent soma and neurite imaging by diffusion MRI (SANDI) is a model analysis method for diffusion that assumes the existence of a cell body in the neural tissue called soma in addition to NODDI.¹¹⁷ Estimation of the soma fraction, if possible, is expected to yield more insights into the activities within the tissue affected by MS, such as the loss of cortical neurons and/or microglial activation.

Currently, SANDI is possible only with MRI systems equipped with exceptionally strong gradients and is dependent on some model assumptions that might not be generally valid, especially in diseased brains.

The immediate disadvantage of more advanced dMRI is that the amount of data required for analysis is much larger than that of DTI, although it is true that the more data there are, the more accurate the analysis can be. SANDI is not commonly used in 3T MRI scanners, which are currently used frequently in clinical practice, since only a limited number of models are capable of performing high b-values and short diffusion times. However, there is a possibility that it will become more widespread in the future with the optimization of the imaging technique and advancements in the imaging technique. In any case, ADCs and FAs in DTI currently used in clinical practice are robust and can be imaged and calculated with any clinical MRI system, although they are not specific enough for any disease or condition; therefore, it is necessary to develop advanced diffusion MRI analysis and apply these methods in clinical practice.

Moreover, the combined analysis of several advanced dMRI techniques may provide a more detailed assessment of the pathogenesis of MS than is possible with conventional

MRI. In addition, advanced dMRI may become a marker for assessing disease severity and determining treatment efficacy in patients with MS. Moreover, dMRI may be useful in differentiating demyelinating diseases, such as MS, from other brain diseases. In particular, differentiation between tumefactive MS and brain tumors is clinically important. Thus, further research on advanced dMRI is necessary in the future.

Conclusion

Several studies have reported that DTI is superior to conventional MRI in the evaluation of NAWM in MS patients; however, advanced dMRI techniques, as described in this review, are more sensitive and have the potential to show specific pathological changes in the microstructure *in vivo*. Clinically, advanced dMRI has been reported to be more sensitive in detecting microstructural changes in the brain that correlate with patient disability¹¹⁸ and in tracking disease progression in NAWM over time, even before clinical symptoms occur.¹¹⁹ In addition, several reports have shown the usefulness of advanced dMRI in NAWM and demyelinating foci. For instance, it is useful in differentiating plaque activity.^{41,120} This indicates that advanced dMRI has clinical promise as an objective and highly sensitive indicator for more accurate staging and subsequent monitoring.

Currently, such advanced dMRI is not possible with any installed MRI system and is not a clinically relevant tool due to hardware and software limitations, complexity, and, in some cases, the need for long analysis times. In addition, most studies on MS patients using advanced dMRI are not sufficient in terms of number and quality to establish evidence. Nevertheless, we believe that dMRI is a promising technique that can noninvasively capture microstructural changes in lesions in the brain and spinal cord and that it will become more clinically useful with the further development of MRI technology.

Funding

This work was supported by JSPS KAKENHI grant numbers 19K08161, 19K17150, 18H02772, and JP16H06280, and AMED grant number JP19lk1010025h9902, the Canada Research Chair in Quantitative Magnetic Resonance Imaging [950-230815], the Canadian Institute of Health Research [CIHR FDN-143263], the Canada Foundation for Innovation [32454, 34824], the Fonds de Recherche du Québec - Santé [28826], the Natural Sciences and Engineering Research Council of Canada [RGPIN-2019-07244], Canada First Research Excellence Fund (IVADO and TransMedTech), the Courtois NeuroMod project, and the Quebec BioImaging Network [5886, 35450].

Conflicts of Interest

The authors declare that they have no conflicts of interest.

References

1. Multiple Sclerosis and Neuromyelitis Optica Guideline Development Committee. Multiple sclerosis and neuromyelitis optica guidelines 2017. Tokyo: Igaku-shoin, 2017. (in Japanese)
2. Polman CH, Reingold SC, Banwell B, et al. Diagnostic criteria for multiple sclerosis: 2010 revisions to the McDonald criteria. *Ann Neurol* 2011; 69:292–302.
3. Miki Y, Grossman RI, Udupa JK, et al. Relapsing-remitting multiple sclerosis: longitudinal analysis of MR images—lack of correlation between changes in T2 lesion volume and clinical findings. *Radiology* 1999; 213:395–399.
4. Barkhof F. The clinico-radiological paradox in multiple sclerosis revisited. *Curr Opin Neurol* 2002; 15:239–245.
5. Cercignani M, Gandini Wheeler-Kingshott C. From micro-to macro-structures in multiple sclerosis: what is the added value of diffusion imaging. *NMR Biomed* 2019; 32:e3888.
6. Filippi M, Iannucci G, Cercignani M, Assunta Rocca M, Pratesi A, Comi G. A quantitative study of water diffusion in multiple sclerosis lesions and normal-appearing white matter using echo-planar imaging. *Arch Neurol* 2000; 57:1017–1021.
7. Werring DJ, Clark CA, Barker GJ, Thompson AJ, Miller DH. Diffusion tensor imaging of lesions and normal-appearing white matter in multiple sclerosis. *Neurology* 1999; 52:1626–1632.
8. Inglese M, Bester M. Diffusion imaging in multiple sclerosis: research and clinical implications. *NMR Biomed* 2010; 23:865–872.
9. Granziera C, Wuerfel J, Barkhof F, et al. MAGNIMS Study Group. Quantitative magnetic resonance imaging towards clinical application in multiple sclerosis. *Brain* 2021; 144:1296–1311.
10. Assaf Y, Ben-Bashat D, Chapman J, et al. High b-value q-space analyzed diffusion-weighted MRI: application to multiple sclerosis. *Magn Reson Med* 2002; 47:115–126.
11. Cohen Y, Assaf Y. High b-value q-space analyzed diffusion-weighted MRS and MRI in neuronal tissues - a technical review. *NMR Biomed* 2002; 15:516–542.
12. Assaf Y, Chapman J, Ben-Bashat D, et al. White matter changes in multiple sclerosis: correlation of q-space diffusion MRI and 1H MRS. *Magn Reson Imaging* 2005; 23:703–710.
13. Lätt J, Nilsson M, Wirestam R, et al. In vivo visualization of displacement-distribution-derived parameters in q-space imaging. *Magn Reson Imaging* 2008; 26:77–87.
14. Farrell JA, Smith SA, Gordon-Lipkin EM, Reich DS, Calabresi PA, van Zijl PC. High b-value q-space diffusion-weighted MRI of the human cervical spinal cord in vivo: feasibility and application to multiple sclerosis. *Magn Reson Med* 2008; 59:1079–1089.
15. Fatima Z, Motosugi U, Hori M, et al. High b-value q-space analyzed diffusion-weighted MRI using 1.5 tesla clinical scanner; determination of displacement parameters in the brains of normal versus multiple sclerosis and low-grade glioma subjects. *J Neuroimaging* 2012; 22:279–284.
16. Mustafi SM, Harezlak J, Kodiweera C, et al. Detecting white matter alterations in multiple sclerosis using advanced diffusion magnetic resonance imaging. *Neural Regen Res* 2019; 14:114–123.
17. Hori M, Fukunaga I, Masutani Y, et al. Visualizing non-Gaussian diffusion: clinical application of q-space imaging and diffusional kurtosis imaging of the brain and spine. *Magn Reson Med Sci* 2012; 11:221–233.
18. Hori M, Yoshida M, Yokoyama K, et al. Multiple sclerosis: Benefits of q-space imaging in evaluation of normal-appearing and periplaque white matter. *Magn Reson Imaging* 2014; 32:625–629.
19. Fujiyoshi K, Hikishima K, Nakahara J, et al. Application of q-space diffusion MRI for the visualization of white matter. *J Neurosci* 2016; 36:2796–2808.
20. Tanikawa M, Nakahara J, Hata J, et al. q-Space Myelin Map imaging for longitudinal analysis of demyelination and remyelination in multiple sclerosis patients treated with fingolimod: A preliminary study. *J Neurol Sci* 2017; 373:352–357.
21. Nakahara J. Visualization of myelin for the diagnosis and treatment monitoring of multiple sclerosis. *Adv Exp Med Biol* 2019; 1190:249–256.
22. Kira JI. q-space Myelin Map imaging: A new imaging technique for treatment evaluation in multiple sclerosis. *J Neurol Sci* 2017; 373:358–359.
23. Cohen Y, Anaby D, Morozov D. Diffusion MRI of the spinal cord: from structural studies to pathology. *NMR Biomed* 2017; 30:e3592.
24. Abdel-Aziz K, Schneider T, Solanky BS, et al. Evidence for early neurodegeneration in the cervical cord of patients with primary progressive multiple sclerosis. *Brain* 2015; 138:1568–1582.
25. Cortese R, Tur C, Prados F, et al. Ongoing microstructural changes in the cervical cord underpin disability progression in early primary progressive multiple sclerosis. *Mult Scler* 2021; 27:28–38.
26. Jensen JH, Helpert JA, Ramani A, Lu H, Kaczynski K. Diffusional kurtosis imaging: the quantification of non-gaussian water diffusion by means of magnetic resonance imaging. *Magn Reson Med* 2005; 53:1432–1440.
27. Helpert JA, Adisetiyo V, Falangola MF, et al. Preliminary evidence of altered gray and white matter microstructural development in the frontal lobe of adolescents with attention-deficit hyperactivity disorder: a diffusional kurtosis imaging study. *J Magn Reson Imaging* 2011; 33:17–23.
28. Setsompop K, Gagoski BA, Polimeni JR, Witzel T, Wedeen VJ, Wald LL. Blipped-controlled aliasing in parallel imaging for simultaneous multislice echo planar imaging with reduced g-factor penalty. *Magn Reson Med* 2012; 67:1210–1224.
29. Sagawa H, Fushimi Y, Nakajima S, et al. Deep learning-based noise reduction for fast volume diffusion tensor imaging: Assessing the noise reduction effect and reliability of diffusion metrics. *Magn Reson Med Sci* 2021; 20:450–456.
30. Murase T, Umeda M, Higuchi T. Investigation of acupuncture-specific BOLD signal changes using multi-band acquisition and deconvolution analysis. *Magn Reson Med Sci* 2021; 20:425–430.
31. Yoshida M, Hori M, Yokoyama K, et al. Diffusional kurtosis imaging of normal-appearing white matter in multiple sclerosis: preliminary clinical experience. *Jpn J Radiol* 2013; 31:50–55.

32. Sahin S, Çam I, Öztürk O, Efendi H, Anık Y, Gundogdu O. White matter evaluation in multiple sclerosis through magnetic resonance kurtosis imaging. *Cureus* 2019; 11:e6424.
33. Raz E, Bester M, Sigmund EE, et al. A better characterization of spinal cord damage in multiple sclerosis: a diffusional kurtosis imaging study. *AJNR Am J Neuroradiol* 2013; 34:1846–1852.
34. Martin AR, Aleksanderek I, Cohen-Adad J, et al. Translating state-of-the-art spinal cord MRI techniques to clinical use: A systematic review of clinical studies utilizing DTI, MT, MWF, MRS, and fMRI. *Neuroimage Clin* 2016; 10:192–238.
35. Bester M, Jensen JH, Babb JS, et al. Non-Gaussian diffusion MRI of gray matter is associated with cognitive impairment in multiple sclerosis. *Mult Scler* 2015; 21:935–944.
36. Takemura MY, Hori M, Yokoyama K, et al. Alterations of the optic pathway between unilateral and bilateral optic nerve damage in multiple sclerosis as revealed by the combined use of advanced diffusion kurtosis imaging and visual evoked potentials. *Magn Reson Imaging* 2017; 39:24–30.
37. Spampinato MV, Kocher MR, Jensen JH, Helpert JA, Collins HR, Hatch NU. Diffusional Kurtosis Imaging of the Corticospinal Tract in Multiple Sclerosis: Association with Neurologic Disability. *AJNR Am J Neuroradiol* 2017; 38:1494–1500.
38. Qian W, Chan KH, Hui ES, Lee CY, Hu Y, Mak HK. Application of diffusional kurtosis imaging to detect occult brain damage in multiple sclerosis and neuromyelitis optica. *NMR Biomed* 2016; 29:1536–1545.
39. Lu P, Yuan T, Liu X, Tian G, Zhang J, Sha Y. Role of diffusional kurtosis imaging in differentiating neuromyelitis optica-related and multiple sclerosis-related acute optic neuritis: Comparison with diffusion-weighted imaging. *J Comput Assist Tomogr* 2020; 44:47–52.
40. De Santis S, Bastiani M, Droby A, et al. Characterizing microstructural tissue properties in multiple sclerosis with diffusion MRI at 7 T and 3 T: The impact of the experimental design. *Neuroscience* 2019; 403:17–26.
41. Thaler C, Kyselyova AA, Faizy TD, et al. Heterogeneity of multiple sclerosis lesions in fast diffusional kurtosis imaging. *PLoS One* 2021; 16:e0245844.
42. Novikov DS, Kiselev VG, Jespersen SN. On modeling. *Magn Reson Med* 2018; 79:3172–3193.
43. Jelescu IO, Palombo M, Bagnato F, Schilling KG. Challenges for biophysical modeling of microstructure. *J Neurosci Methods* 2020; 344:108861.
44. Zhang H, Schneider T, Wheeler-Kingshott CA, Alexander DC. NODDI: practical in vivo neurite orientation dispersion and density imaging of the human brain. *Neuroimage* 2012; 61:1000–1016.
45. Kamiya K, Hori M, Aoki S. NODDI in clinical research. *J Neurosci Methods* 2020; 346:108908.
46. Caverzasi E, Papinutto N, Castellano A, et al. Neurite orientation dispersion and density imaging color maps to characterize brain diffusion in neurologic disorders. *J Neuroimaging* 2016; 26:494–498.
47. Hagiwara A, Kamagata K, Shimoji K, et al. White matter abnormalities in multiple sclerosis evaluated by quantitative synthetic MRI, diffusion tensor imaging, and neurite orientation dispersion and density imaging. *AJNR Am J Neuroradiol* 2019; 40:1642–1648.
48. Hagiwara A, Hori M, Yokoyama K, et al. Analysis of white matter damage in patients with multiple sclerosis via a novel in vivo MR method for measuring myelin, axons, and G-ratio. *AJNR Am J Neuroradiol* 2017; 38:1934–1940.
49. Calabrese M, Castellaro M, Bertoldo A, et al. Epilepsy in multiple sclerosis: The role of temporal lobe damage. *Mult Scler* 2017; 23:473–482.
50. Granberg T, Fan Q, Treaba CA, et al. In vivo characterization of cortical and white matter neuroaxonal pathology in early multiple sclerosis. *Brain* 2017; 140:2912–2926.
51. Spanò B, Giulietti G, Pisani V, et al. Disruption of neurite morphology parallels MS progression. *Neurol Neuroimmunol Neuroinflamm* 2018; 5:e502.
52. Lakhani DA, Schilling KG, Xu J, Bagnato F. Advanced multicompartiment diffusion MRI models and their application in multiple sclerosis. *AJNR Am J Neuroradiol* 2020; 41:751–757.
53. Caverzasi E, Cordano C, Zhu AH, et al. Imaging correlates of visual function in multiple sclerosis. *PLoS One* 2020; 15:e0235615.
54. Collorone S, Prados F, Kanber B, et al. Brain microstructural and metabolic alterations detected in vivo at onset of the first demyelinating event. *Brain* 2021; 144:1409–1421.
55. Lu PJ, Barakovic M, Weigel M, et al. GAMER-MRI in multiple sclerosis identifies the diffusion-based microstructural measures that are most sensitive to focal damage: A Deep-Learning-Based Analysis and Clinico-Biological Validation. *Front Neurosci* 2021; 15:647535.
56. Sacco S, Caverzasi E, Papinutto N, et al. University of California, San Francisco MS-EPIC Team. Neurite orientation dispersion and density imaging for assessing acute inflammation and lesion evolution in MS. *AJNR Am J Neuroradiol* 2020; 41:2219–2226.
57. By S, Xu J, Box BA, Bagnato FR, Smith SA. Application and evaluation of NODDI in the cervical spinal cord of multiple sclerosis patients. *Neuroimage Clin* 2017; 15:333–342.
58. Collorone S, Cawley N, Grussu F, et al. Reduced neurite density in the brain and cervical spinal cord in relapsing-remitting multiple sclerosis: A NODDI study. *Mult Scler* 2020; 26:1647–1657.
59. Grussu F, Schneider T, Tur C, et al. Neurite dispersion: a new marker of multiple sclerosis spinal cord pathology? *Ann Clin Transl Neurol* 2017; 4:663–679.
60. Gong T, Tong Q, He H, Sun Y, Zhong J, Zhang H. MTE-NODDI: Multi-TE NODDI for disentangling non-T2-weighted signal fractions from compartment-specific T2 relaxation times. *Neuroimage* 2020; 217:116906.
61. Hori M, Kamiya K, Murata K. Technical basics of diffusion-weighted imaging. *Magn Reson Imaging Clin N Am* 2021; 29:129–136.
62. Novikov DS, Fieremans E, Jespersen SN, Kiselev VG. Quantifying brain microstructure with diffusion MRI: Theory and parameter estimation. *NMR Biomed* 2019; 32:e3998.
63. Fieremans E, Burcaw LM, Lee HH, Lemberskiy G, Veraart J, Novikov DS. In vivo observation and biophysical interpretation of time-dependent diffusion in human white matter. *Neuroimage* 2016; 129:414–427.

64. Lee HH, Papaioannou A, Novikov DS, Fieremans E. In vivo observation and biophysical interpretation of time-dependent diffusion in human cortical gray matter. *Neuroimage* 2020; 222:117054.
65. Kiselev VG. Fundamentals of diffusion MRI physics. *NMR Biomed* 2017; 30:e3602.
66. Novikov DS, Veraart J, Jelescu IO, Fieremans E. Rotationally-invariant mapping of scalar and orientational metrics of neuronal microstructure with diffusion MRI. *Neuroimage* 2018; 174:518–538.
67. Reisert M, Kiselev VG, Dhital B. A unique analytical solution of the white matter standard model using linear and planar encodings. *Magn Reson Med* 2019; 81:3819–3825.
68. Buyukturkoglu K, Fleyser L, Byrd D, Morgello S, Inglese M. Diffusion kurtosis imaging shows similar cerebral axonal damage in patients with HIV infection and multiple Sclerosis. *J Neuroimaging* 2018; 28:320–327.
69. Margoni M, Petracca M, Schiavi S, et al. Axonal water fraction as marker of white matter injury in primary-progressive multiple sclerosis: a longitudinal study. *Eur J Neurol* 2019; 26:1068–1074.
70. Ngamsombat C, Tian Q, Fan Q, et al. Axonal damage in the optic radiation assessed by white matter tract integrity metrics is associated with retinal thinning in multiple sclerosis. *Neuroimage Clin* 2020; 27:102293.
71. de Kouchkovsky I, Fieremans E, Fleysher L, Herbert J, Grossman RI, Inglese M. Quantification of normal-appearing white matter tract integrity in multiple sclerosis: a diffusion kurtosis imaging study. *J Neurol* 2016; 263:1146–1155.
72. Jelescu IO, Zurek M, Winters KV, et al. In vivo quantification of demyelination and recovery using compartment-specific diffusion MRI metrics validated by electron microscopy. *Neuroimage* 2016; 132:104–114.
73. Fieremans E, Jensen JH, Helpert JA, et al. Diffusion distinguishes between axonal loss and demyelination in brain white matter. Proceedings of the 20th annual meeting and exhibition of ISMRM, Melbourne, 2012.
74. Guglielmetti C, Veraart J, Roelant E, et al. Diffusion kurtosis imaging probes cortical alterations and white matter pathology following cuprizone induced demyelination and spontaneous remyelination. *Neuroimage* 2016; 125:363–377.
75. Jelescu IO, Veraart J, Fieremans E, Novikov DS. Degeneracy in model parameter estimation for multi-compartmental diffusion in neuronal tissue. *NMR Biomed* 2016; 29:33–47.
76. Andersson M, Kjer HM, Rafael-Patino J, et al. Axon morphology is modulated by the local environment and impacts the noninvasive investigation of its structure-function relationship. *Proc Natl Acad Sci U S A* 2020; 117:33649–33659.
77. Lee HH, Yaros K, Veraart J, et al. Along-axon diameter variation and axonal orientation dispersion revealed with 3D electron microscopy: implications for quantifying brain white matter microstructure with histology and diffusion MRI. *Brain Struct Funct* 2019; 224:1469–1488.
78. Coronado-Leija R, Lee H-H, Fieremans E, Novikov DS. Characterizing time-dependent diffusion in the extra-axonal space of white matter for axon loss and demyelination. Proceedings of the 2021 annual meeting and exhibition of ISMRM, online, 2021.
79. Shemesh N, Jespersen SN, Alexander DC, et al. Conventions and nomenclature for double diffusion encoding NMR and MRI. *Magn Reson Med* 2016; 75:82–87.
80. Topgaard D. Multidimensional diffusion MRI. *J Magn Reson* 2017; 275:98–113.
81. Shemesh N, Adiri T, Cohen Y. Probing microscopic architecture of opaque heterogeneous systems using double-pulsed-field-gradient NMR. *J Am Chem Soc* 2011; 133:6028–6035.
82. Cory D, Garroway A, Miller J. Applications of spin transport as a probe of local geometry. *Polymer Prepr* 1990; 31:149–151.
83. Jespersen SN, Lundell H, Sønderby CK, Dyrby TB. Orientationally invariant metrics of apparent compartment eccentricity from double pulsed field gradient diffusion experiments. *NMR Biomed* 2013; 26:1647–1662.
84. Yang G, Tian Q, Leuze C, Wintermark M, McNab JA. Double diffusion encoding MRI for the clinic. *Magn Reson Med* 2018; 80:507–520.
85. Mori S, van Zijl PC. Diffusion weighting by the trace of the diffusion tensor within a single scan. *Magn Reson Med* 1995; 33:41–52.
86. Westin CF, Knutsson H, Pasternak O, et al. Q-space trajectory imaging for multidimensional diffusion MRI of the human brain. *Neuroimage* 2016; 135:345–362.
87. Andersen KW, Lasič S, Lundell H, et al. Disentangling white-matter damage from physiological fibre orientation dispersion in multiple sclerosis. *Brain Commun* 2020; 2:fcaa077.
88. Lee J, Hyun JW, Lee J, et al. So you want to image myelin using MRI: An overview and practical guide for myelin water imaging. *J Magn Reson Imaging* 2021; 53:360–373.
89. Hagiwara A, Warntjes M, Hori M, et al. SyMRI of the brain: Rapid Quantification of Relaxation Rates and Proton Density, With synthetic MRI, automatic brain segmentation, and myelin measurement. *Invest Radiol* 2017; 52:647–657.
90. van der Weijden CWJ, García DV, Borra RJH, et al. Myelin quantification with MRI: A systematic review of accuracy and reproducibility. *Neuroimage* 2021; 226:117561.
91. Stikov N, Campbell JS, Stroh T, et al. In vivo histology of the myelin g-ratio with magnetic resonance imaging. *Neuroimage* 2015; 118:397–405.
92. Stikov N, Campbell JS, Stroh T, et al. Quantitative analysis of the myelin g-ratio from electron microscopy images of the macaque corpus callosum. *Data Brief* 2015; 4:368–373.
93. Mohammadi S, Carey D, Dick F, et al. Whole-brain in-vivo measurements of the axonal G-ratio in a group of 37 healthy volunteers. *Front Neurosci* 2015; 9:441.
94. Duval T, Le Vy S, Stikov N, et al. g-Ratio weighted imaging of the human spinal cord in vivo. *Neuroimage* 2017; 145:11–23.
95. Hori M, Hagiwara A, Fukunaga I, et al. Application of quantitative microstructural MR imaging with atlas-based analysis for the spinal cord in cervical spondylotic myelopathy. *Sci Rep* 2018; 8:5213.
96. Hildebrand C, Hahn R. Relation between myelin sheath thickness and axon size in spinal cord white matter of some vertebrate species. *J Neurol Sci* 1978; 38:421–434.
97. Albert M, Antel J, Brück W, Stadelmann C. Extensive cortical remyelination in patients with chronic multiple sclerosis. *Brain Pathol* 2007; 17:129–138.

98. RUSHTON WA. A theory of the effects of fibre size in medullated nerve. *J Physiol* 1951; 115:101–122.
99. Kamagata K, Zalesky A, Yokoyama K, et al. MR g-ratio-weighted connectome analysis in patients with multiple sclerosis. *Sci Rep* 2019; 9:13522.
100. Waxman SG. Determinants of conduction velocity in myelinated nerve fibers. *Muscle Nerve* 1980; 3:141–150.
101. Dean DC, O’Muircheartaigh J, Dirks H, et al. Mapping an index of the myelin g-ratio in infants using magnetic resonance imaging. *Neuroimage* 2016; 132:225–237.
102. Ashburner J, Friston KJ. Voxel-based morphometry—the methods. *Neuroimage* 2000; 11:805–821.
103. Tudorascu DL, Karim HT, Maronge JM, et al. Reproducibility and bias in healthy brain segmentation: Comparison of two popular neuroimaging platforms. *Front Neurosci* 2016; 10:503.
104. De Leener B, Lévy S, Dupont SM, et al. SCT: Spinal Cord Toolbox, an open-source software for processing spinal cord MRI data. *Neuroimage* 2017; 145:24–43.
105. De Leener B, Fonov VS, Collins DL, Callot V, Stikov N, Cohen-Adad J. PAM50: Unbiased multimodal template of the brainstem and spinal cord aligned with the ICBM152 space. *Neuroimage* 2018; 165:170–179.
106. Martin M. Measuring restriction sizes using diffusion weighted magnetic resonance imaging: a review. *Magn Reson Insights* 2013; 6:59–64.
107. Wu D, Martin LJ, Northington FJ, Zhang J. Oscillating gradient diffusion MRI reveals unique microstructural information in normal and hypoxia-ischemia injured mouse brains. *Magn Reson Med* 2014; 72:1366–1374.
108. Novikov DS, Jensen JH, Helpert JA, Fieremans E. Revealing mesoscopic structural universality with diffusion. *Proc Natl Acad Sci U S A* 2014; 111:5088–5093.
109. Xu J. Probing neural tissues at small scales: Recent progress of oscillating gradient spin echo (OGSE) neuroimaging in humans. *J Neurosci Methods* 2021; 349:109024.
110. Baron CA, Kate M, Gioia L, et al. Reduction of diffusion-weighted imaging contrast of acute ischemic stroke at short diffusion times. *Stroke* 2015; 46:2136–2141.
111. Andica C, Hori M, Kamiya K, et al. Spatial restriction within intracranial epidermoid cysts observed using short diffusion-time diffusion-weighted imaging. *Magn Reson Med Sci* 2018; 17:269–272.
112. Maekawa T, Kamiya K, Murata K, Feiweier T, Hori M, Aoki S. Time-dependent diffusion in transient splenial lesion: Comparison between oscillating-gradient spin-echo measurements and monte-carlo simulation. *Magn Reson Med Sci* 2021; 20:227–230.
113. Iima M, Yamamoto A, Kataoka M, et al. Time-dependent diffusion MRI to distinguish malignant from benign head and neck tumors. *J Magn Reson Imaging* 2019; 50:88–95.
114. Xu J, Jiang X, Li H, et al. Magnetic resonance imaging of mean cell size in human breast tumors. *Magn Reson Med* 2020; 83:2002–2014.
115. Lemberskiy G, Rosenkrantz AB, Veraart J, Taneja SS, Novikov DS, Fieremans E. Time-dependent diffusion in prostate cancer. *Invest Radiol* 2017; 52:405–411.
116. By S, Smith SA, Schilling KG, et al. Oscillating Gradient Spin Echo (OGSE) diffusion tensor imaging of the human spinal cord: application to multiple sclerosis. *Proceedings of the annual meeting of ISMRM, Paris, 2018.*
117. Palombo M, Ianus A, Guerreri M, et al. SANDI: A compartment-based model for non-invasive apparent soma and neurite imaging by diffusion MRI. *Neuroimage* 2020; 215:116835.
118. Johnson D, Ricciardi A, Brownlee W, et al. Comparison of neurite orientation dispersion and density imaging and two-compartment spherical mean technique parameter maps in multiple sclerosis. *Front Neurol* 2021; 12:662855.
119. Toschi N, De Santis S, Granberg T, et al. Evidence for progressive microstructural damage in early multiple sclerosis by multi-shell diffusion magnetic resonance imaging. *Neuroscience* 2019; 403:27–34.
120. Oladosu O, Liu WQ, Pike BG, Koch M, Metz LM, Zhang Y. Advanced analysis of diffusion tensor imaging along with machine learning provides new sensitive measures of tissue pathology and intra-lesion activity in multiple sclerosis. *Front Neurosci* 2021; 15:634063.